MATTER: International Journal of Science and Technology
ISSN 2454-5880

Żur et al., 2024

Volume 10, pp. 48-74

Received: 02nd August 2023

Revised: 18th July 2023, 22nd December 2023, 29th December 2023, 16th January 2024, 29th January 2024

Accepted: 03rd August 2023

Date of Publication: 15th June 2024

DOI- https://doi.org/10.20319/mijst.2024.10.4874

This paper can be cited as: Żur, P., Żur, A., Michalski, P. & Baier, A. (2024). Strain Gauge Testing of 3D-Printed CFRP Sandwich Structure. MATTER: International Journal of Science and Technology, 10, 48-74.

STRAIN GAUGE TESTING OF 3D-PRINTED CFRP SANDWICH STRUCTURE

Paweł Żur
Department of Engineering Processes Automation And Integrated Manufacturing Systems, Faculty of Mechanical Engineering, Silesian University of Technology, Gliwice, Poland
pawel.zur@polsl.pl

Alicja Żur
Department of Engineering Processes Automation And Integrated Manufacturing Systems, Faculty of Mechanical Engineering, Silesian University of Technology, Gliwice, Poland
alicja.zur@polsl.pl

Piotr Michalski
Department of Engineering Processes Automation And Integrated Manufacturing Systems, Faculty of Mechanical Engineering, Silesian University of Technology, Gliwice, Poland
piotr.michalski@polsl.pl

Andrzej Baier
Department of Engineering Processes Automation And Integrated Manufacturing Systems, Faculty of Mechanical Engineering, Silesian University of Technology, Gliwice, Poland
andrzej.baier@polsl.pl

Abstract

In this article, the authors present composite sandwich-type CFRP structures and a study of their properties by strain gauge testing. The paper presents the modeling of a parameterized elementary

unit serving as the core of a 3D printed structure using Fused Deposition Modelling (FDM) technology. The properties of these structures with different outer layers made of pure epoxy resin and resin with 10% and 20% carbon fiber powder were then investigated. Based on the results of the strain gauge tests, material models were reconstructed for each resin layer, which can be used in computer FEM studies of more complex components. As an application example, a strength analysis of the driver's seat of a Greenpower car made with printed sandwich structures coated with carbon fiber powder resin was conducted.

Keywords

3D Printing, Carbon Fiber, CFRP Composite, Sandwich Structure, Strain Gauge Testing

1. Introduction

The purpose of the study was to investigate strain gauging of innovative compo-site sandwich structures. The premise of the study is to model a scalable elementary unit that can then be multiplied to form the core of a sandwich structure. In this article, the authors examine the mechanical properties of such elements using resistance strain gauge testing.

In recent years, the importance of Continuous Fiber Reinforced Thermoplastic Composites (CFRTPCs) has increased considerably. Numerous industrial requirements for new materials led to the development of innovative manufacturing and design forms. New composite manufacturing technologies and new composite technologies allow traditional materials to be replaced by light structures and are not inferior in mechanical properties to traditional materials.

As described in this paper, a new type of CFRP materials and a new composite manufacturing approach have been developed. - 3D print in Fused Deposition Modelling (FDM) technology considering the print to be a lightweight structure reinforced with epoxy resin layer with the addition of carbon fiber powder. Innovation in the manufacturing process is essential and urgent to further develop and apply CFRTPC material. [1-3]

At present, FDM is used not only for visual aids, conceptual models, and prototypes but also for manufacturing of functional parts. 3D printing technology based on material extrusion can be used for printing multiple materials and multiple color printing of plastics, food, and even living cells. The technology is widely used because it is low in cost and can be built in fully functional parts. 3D printing technology, also known as additive manufacturing, involves producing a given object or component by adding material layer by layer and creating a three-dimensional (3D)

structure. It reduces the cost of assembly by producing complex geometry and flexible functional components from STL files by depositing two-dimensional (2D) layers of melted polymeric material on a build platform. Using CAD (Computer Aided Design) software, it is needed to create and design appropriate print models in advance. [4, 5, 6, 7]

Low-precision is a relative term, but some applications do not require high-precision (prototypes or displays), in order for FDM to be more acceptable in the industry for mass production of printed parts, accuracy is the fundamental requirement. Many researchers have analyzed various control parameters to achieve the desirable characteristics of the component and have also been working on optimizing the process parameters [4, 8]. Several factors affect the quality of the final elements. – Printing temperature, printing speed, layer height, print architecture (infill pattern), cooling rate. [1, 9]

Currently, there are a number of articles in which the authors study the properties of particular predefined filling structures of 3D prints. In the notable majority of these articles, they treat the effect of filling and other parameters on mechanical properties. Modeling custom structures and using them in 3D printing is no longer such a popular topic. The topic has been addressed by, for example: Audibert et al. [10] in which the authors study shapes built from bone geometry, as well as author Bodaghi et al. [11] where the aim of that paper was to introduce auxetic meta-sandwiches printing technology for reversible energy absorption applications.

Saufi et al. [12] proposed using a shape inspired by nature - the starfish. The bio-inspired structure has been studied for its ability to absorb energy and high strength.

The topic addressed in this article - parametric spatial structure reinforced with carbon fiber dust and epoxy resin, is an innovative and previously unaddressed issue. Currently, new composite manufacturing technologies combined with new materials can replace traditional materials with light structures with similar resistance. These structures allow the weight and materials needed for the production of the elements to be reduced [13, 14].

Designing structures to improve load bearing capability with reduction of weight and impact resistance is one of the multidisciplinary research fields, with potential applications in a wide variety of areas, such as automotive, space, civil, and biomedical, among others. Advanced scalable technologies, such as 3D printing, can be used to explore the mechanical behavior of various predictive complex geometric shapes, to create innovative engineering materials. [15, 16, 17].

Composite materials are materials composed of at least two materials (phases) with different properties and have properties superior to each component separately, but also superior to those derived from a simple summarization of these properties [5, 14]. Examples of such materials are polymers reinforced with carbon fibers. They are widely used in the aerospace industry due to their high resistance, corrosion resistance, and fatigue resistance. [18] It is a well-known practice to add various types of fillers to epoxy resin to enhance its strength or modify selected properties [14, 19-25]. Among the fillers used are silica, quartz flour, glass or carbon fiber dust, short fibers, and graphene. However, the authors propose a new approach by mixing carbon fiber powder into the epoxy resin.

Sandwich composite structures are widely used in weight-restricted applications, such as in the automotive or aerospace industry. Researchers have developed better mechanically resistant alternative materials, such as hexagonal and reintroduced honeycomb cores, and the structure of lattice trusses and cell auxetic structures. However, these structures have several serious limitations, mainly manufacturing methods – eg. Extrusion, forming and corrugation [26-30]. Other studies have shown that it is highly challenging to manufacture lattice structures, e.g. cubic diamond or gyroid structure, by traditional subtractive methods. Using 3D printing could help overcome these difficulties and suggests new ways of manufacturing the support structures and cores [31-37].

In this article, the authors also propose an innovative method to manufacture such composites using 3D printing with FDM technology. The printed cores of the structure are then coated with a layer of epoxy resin along with the admixture of 10% and 20% carbon fiber powder. The resulting CFRP composite allows for diversified applications: 3D printing makes it possible to produce a core of any shape, while the res-in with the addition of carbon fiber powder, unlike classical laminates, also allows uniform coverage of surfaces with almost any degree of complexity and refraction.

In the next part of the study, strain gauge tests were performed. The principle of the resistance strain gauge is based on the strain gauge effect of the resistance material. This effect was first observed in 1856 by William Thomson. It consists of a change in the electrical resistance of the material with a change in its length. The sensor's resistance material deforms during operation. In the linear range of the stress characteristics, as a function of the elongation of the elastic element, the deformation is reversible, and the resistance function is linear. [38]

Strain gauges can be made of many metals and alloys. The most common are constantan (an alloy of copper and nickel in a ratio of 3:2) and nichrome (an alloy of 80% nickel and 20% chromium). The most important advantages of strain gauge testing include its small size, and therefore the ability to take measurements in hard-to-reach places, high measurement accuracy, and relatively low cost. However, this method is not without its disadvantages, which certainly include the long preparation time for the test that involves proper surface preparation and sticking of the strain gauges, as well as the disposability of the strain gauges used, as once a strain gauge is stuck on, it cannot be peeled off without damaging it. [38, 39]

The purpose of this study of sandwich CFRP structures is to implement them as an infill for the driver's seat in a Greenpower electric car. Silesian Greenpower is the students' interfaculty project that focuses on the design and construction of electric racing vehicles. However, the Greenpower car is not a regular EV. It is a one-person lightweight construction. The Greenpower car is designed for specific type of races and is not admitted to road traffic. The main restriction in the design of the car is imposed by the organizers, the power source, and type of the motor driving the car, which increases the competition level and equalizes the chances of teams. Greenpower electric vehicles are characterized by low weight (about 90 kg without the driver) and rather low speeds (about 50 km/h), so they do not require such exorbitant strength properties and thermal resistance, and more critical here is the low weight and the possibility of unit production of custom parts at low cost. [40, 41]

The driver's seat is a car component that has several tasks, primarily to ensure the driver's safe position in the car but also to provide comfort while driving. Therefore, it is ideal to design a seat for a particular driver to best suit his or her ergonomics. This approach has one disadvantage - the cost of making such a unitary seat increases significantly due to the uniqueness of the component. The use of structures and methods studied in this article will reduce the cost of manufacturing such a seat. In addition, such structures can be used in the design of damping suspension components, such as bushings, using more resilient materials. [13, 42, 43]

2. Materials and Methods

In this section, the model and sample preparation process and the tests test methodology of the conducted are described. First, the modelling of the core structure was prepared for the Finite Element Method (FEM) analysis. The obtained CAD model was further used to prepare a sandwich

structure composite. The core of the structure was 3D printed and laminated. The prepared samples were subjected to strain gauge testing. Then the material model was retrieved on the experimentally acquired data. Lastly, an FEM analysis of the driver's seat has been conducted.

2.1. CAD Model

The first step of this study was preparing a CAD model of the support structure geometry. For this purpose, the Siemens NX 12 program was used. The main idea was to prepare a model of an elementary unit, designed with the help of parameterized variables. The use of parameterization in the model allows to adjust the size and change the geometry within a given range. Two geometries with truss characteristics were pro-posed - type one with vertical supports only, and type two with additional diagonal supports. The geometry of the models is shown in the figure. The models consisted of a hexagonal cube with the following variables: height (h), thickness of bases (b), and thickness of supports (s), both vertical and diagonal supports. The elements used in the subsequent tests were 8x8x8 mm, the thickness of the bases was 0.5 mm, while the thickness of the supports was 1.5 mm. Additional diagonal support was created using a circular array with the element spaced every 90 degrees. This ensures that the diagonal supports on opposite walls are arranged perpendicular to each other.

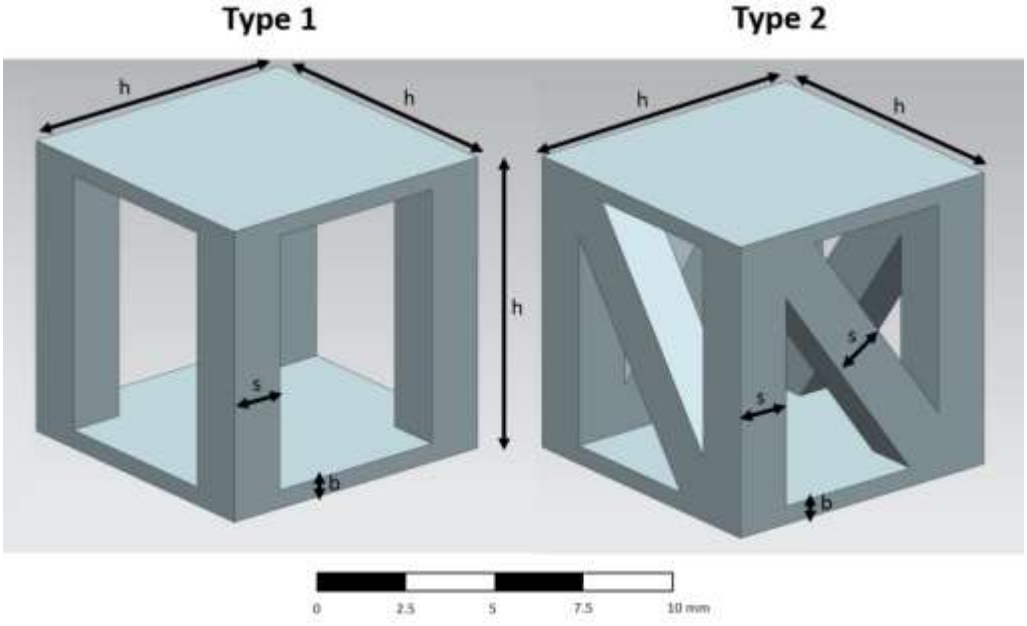

Figure 1: *Comparison of Two Types of Elementary Units along with Scalable Parameters: h – Height, s – Support Thickness, b – Base Thickness*

(Source: Author's Own Illustration)

The elementary units were used to create the core structure of a sandwich-type element. Also, two variants of the core were proposed - consisting of one or two layers of elementary units. To create the infill, an elementary unit was multiplied using the Pattern Feature option. A grid of 160 elements was created, 16 by 10 elements with 2 mm spacing between cubes. For a model with two layers, the number of elements was doubled. Additionally, two thin layers of 0.5 mm thickness were added as bonding surfaces. The size of the modeled core structure is 158x98x9 mm for the model with one layer and 158x98x17 mm for the model with two layers of elements. A comparison of the prepared core models is shown in Figure 1 above and in Table 1 below.

Table 1: *Comparison of Sandwich Core Structure Types*

	Structure A	**Structure B**	**Structure C**
Elementary unit	Type 1	Type 2	Type 1
Number of units	160	160	320

(Source: Author's Own Illustration)

As can be seen from the table above and the data on the weight of each sample, structures with additional diagonal support are heavier than samples without this support - for samples with one layer the difference is 30%, while for samples with two layers the difference is 40% in weight.

2.2. Finite Element Method Analysis

In the next step, the designed structures were subjected to FEM strength testing. For this purpose, Ansys Workbench 19.2 software with the Nastran calculation module was used. Static Structural was selected as the test type. The material adopted for the FEM analysis was Ultra PLA by Noctua. The following manufacturer data were entered for the material constants: Young's modulus – 2,65 GPa, density – 1.3 g/cm3 and Poisson's ratio 0.33. Next, a mesh was created with an element size of 4 mm applied for outer layers. The next step was the task of setting the boundary conditions of the test, simulation of 3-point bending of the plates. The element was supported from below on the two edges along the width of the element which were offset by 10 mm from the edge of the sample. One fixed support and one sliding support were used (1 degree of freedom was left free – rotating along Y axis). A circle with a diameter of 50 mm was drawn on the upper surface, to which a force of 200 N was applied. The single layer element prepared for the FEM testing is shown in Figure 2. Analogous boundary conditions were used for all types of tested structures.

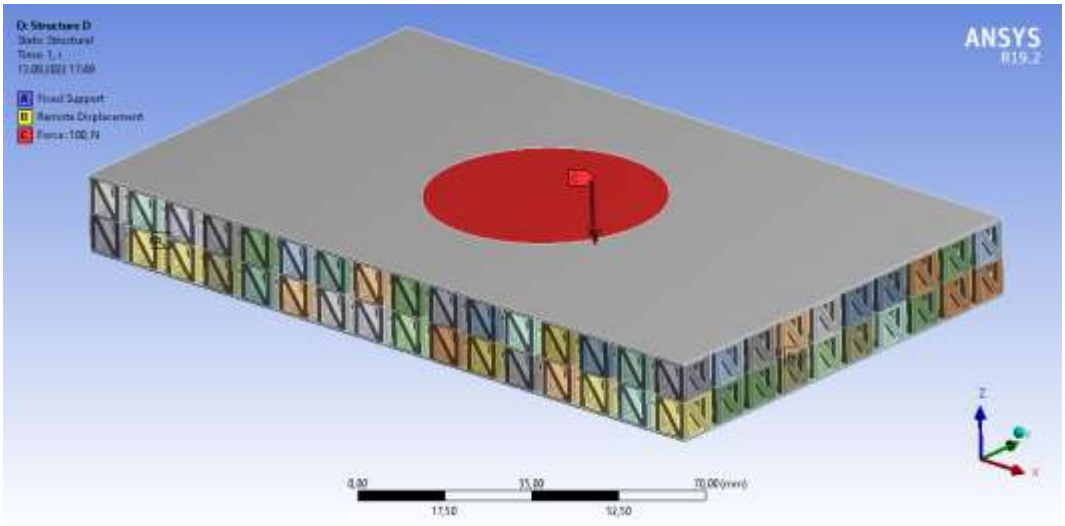

Figure 2: *Double Layer Element (Structure D) Prepared for the FEM Analysis*

(Source: Author's Own Illustration)

2.3. 3D Printing and composite fabrication

The components designed and discussed in the previous two subsections were then printed using FDM (Fused Deposition Modelling) technology on a Prusa MK3S printer. The material chosen for printing was PLA (Polylactic Acid), and the filament used was Noctua's Ultra PLA. The parameters used are shown in Table 2.

Table 2: *3D Printing Parameters*

Parameter	**Value**
Printing temperature	210°C
Heatbed temperature	60°C
Layer height	0.2 mm
Nozzle diameter	0.4 mm
Cooling rate	100%
Number of outlines	2

(Source: Author's Own Illustration)

PLA is one of the widely used thermoplastics in FDM. PLA is increasingly used as a biodegradable thermoplastic. In addition, the process of rapid prototyping with PLA requires less energy and a lower temperature. [1]

The elements are intended to be applied in the Silesian Greenpower electric race car. However, the only heat in the car is generated by the electric motor, which doesn't generate any fumes and is located far away from the seat and has no influence on the degradation of the seat material. Therefore, high-temperature performance is not required in this specific application.

The printed samples were then laminated. For this purpose, LG700 epoxy resin with HG700 hardener from GRM Systems was used. This epoxy system is suitable for both RTM and manual lamination. It is characterized by very low viscosity, good heat resistance, very flexible and strong veneers. Epoxy resin LG700 with hardener HG700 has a 25 minutes processability time [44]. The resin was mixed with the hardener in a weight ratio of 100:35, and then the addition of carbon fiber powder was mixed in different ratios – 10% and 20% by weight. Selected carbon fiber powder was from Easy Composites. It is compatible with different resins – epoxy, polyester, vinylester and polyurethane. It has fiber diameter of 7.5 µm and fiber length of 100 µm. It has the density of 1800 kg/m3. This carbon fiber powder is characterized by tensile strength of 3150 MPa and Young's modulus of 200 GPa [45]. The microscope image of the applied car-bon fiber powder is presented in Figure 3 below. The image was taken using an optical microscope with a magnification of 40 times. It is visible, that the powder consists of very short fibers.

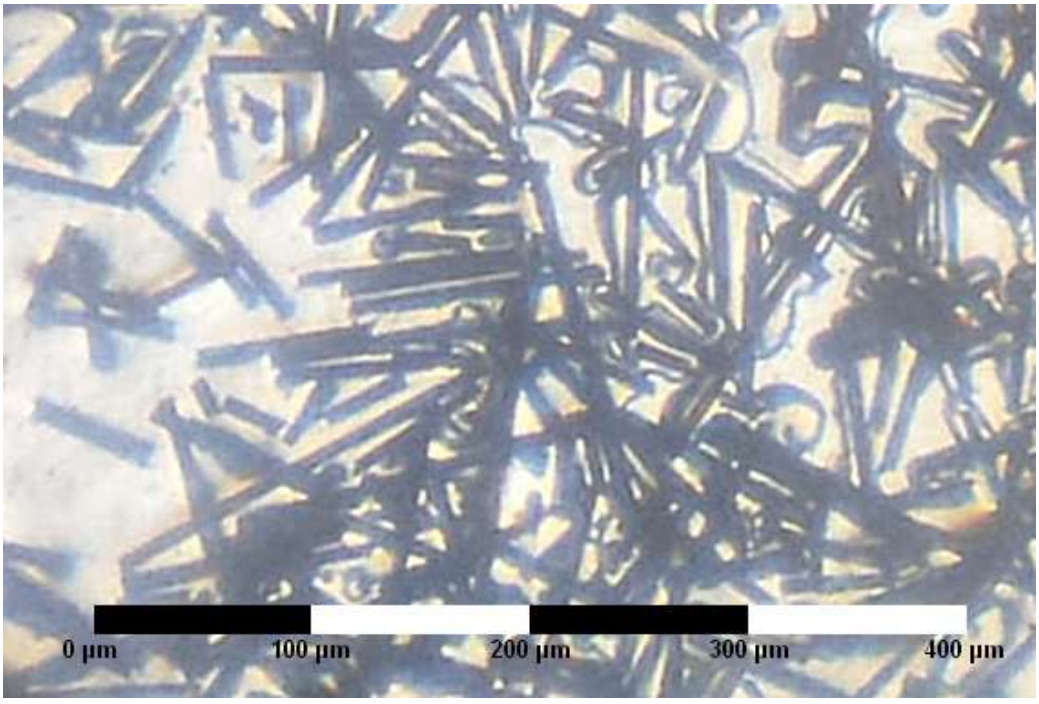

Figure 3: *Microscope Image of Carbon Fiber Powder*

(Source: Author's Own Illustration)

Addition of carbon fiber powder can significantly improve the mechanical properties of the resin. It increases tensile strength and modulus and electrical conductivity. It upgrades thermos-dimensional stability of the produced parts. Also, very high tensile strength and isotropic orientation it reduces shrinkage of the composite. Carbon fiber powder addition was 10% and 20% by weight. The carbon fiber powder was used as a reinforcing additive. Two samples without the addition of carbon fiber powder were also left as reference samples. A summary of all the samples made is shown in the Table 3 below.

Table 3: *Samples Prepared for Strain Gauge Testing*

Sample	**Core structure**	**Coating**
1	Structure A	No coating
2	Structure B	No coating
3	Structure A	Pure epoxy resin LG700
4	Structure B	Pure epoxy resin LG700
5	Structure A	LG700 + 10% carbon fiber powder
6	Structure B	LG700 + 10% carbon fiber powder
7	Structure A	LG700 + 20% carbon fiber powder
8	Structure B	LG700 + 20% carbon fiber powder

(Source: Author's Own Illustration)

For each laminate layer, 10 g of resin mixture was provided, thus obtaining an ap-proximately 1 mm laminate layer on each side of the printed structure. The sample prepared for further testing is shown in Figure 4. The liquid mixture of epoxy and car-bon fiber powder was poured onto the surface of the 3D-printed core. The epoxy resin has self-leveling properties, therefore then the samples were placed on a flat surface to ensure even distribution of the laminate and a smooth surface. Samples were laminated manually. The authors were considering vacuum laminating, but as there was no requirement to press the resin into standard carbon fiber fabric, they chose the simpler method.

Figure 4: *Sample 6 prepared for the strain gauge testing [own illustration]*

Then TF-5 resistance strain gauges with a gain parameter k of 2.15 and a resistance R of 120 Ohms were attached to the samples. The strain gauges were attached 1 strain gauge per sample - in the center of the lower surface, which is shown in Figure 5 below.

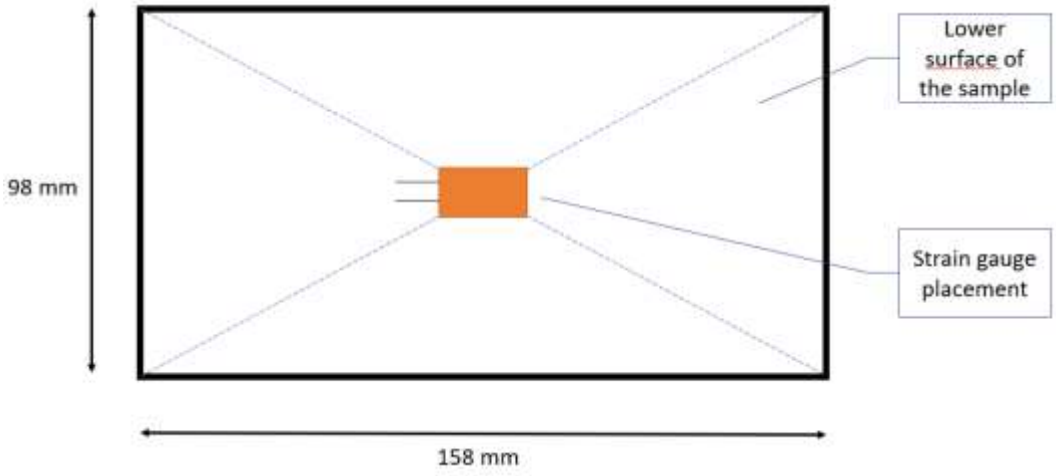

Figure 5: *Placement of the strain gauge on the sample [own illustration]*

2.4. Strain Gauge Testing

In the next stage, the manufactured samples were subjected to strain gauge tests. For this purpose, a test stand equipped with a pneumatic actuator, support elements, sensors, and control software was prepared. The strain gauge test stand is shown in Figure 6.

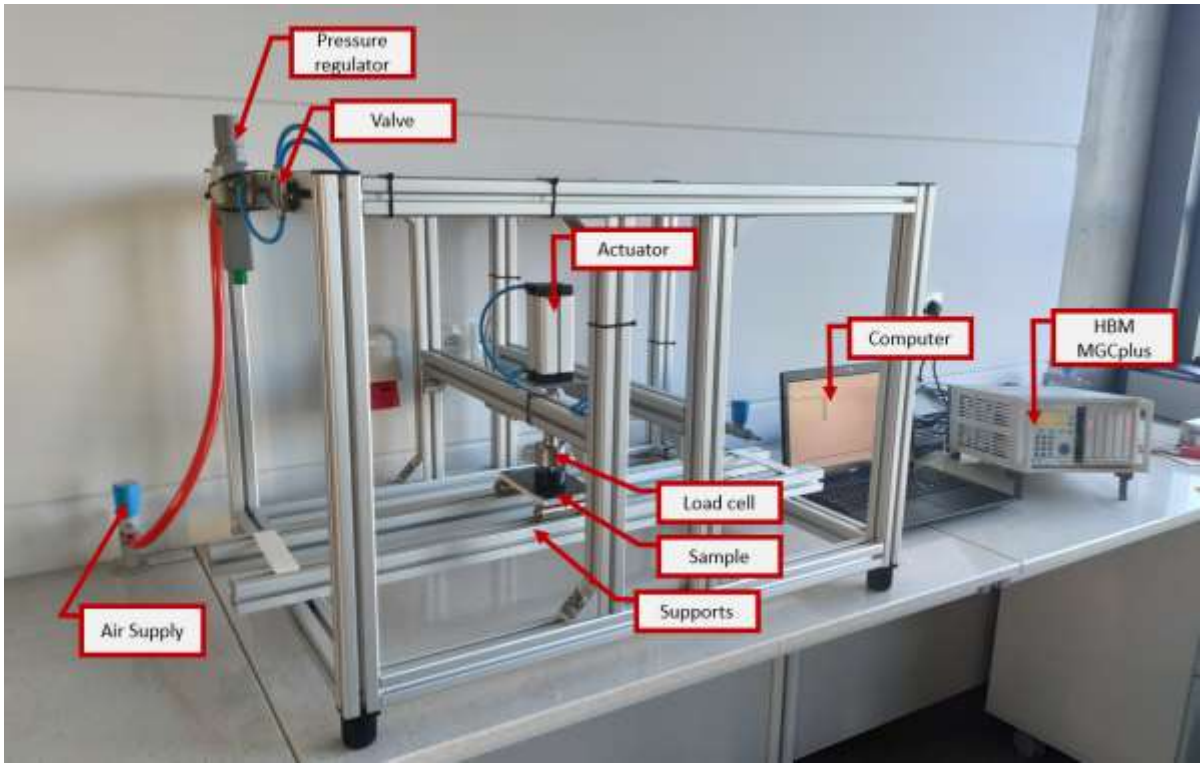

Figure 6: *Strain Gauge Test Stand [own illustration]*

The workstation used an actuator with a stroke of 100 mm, a piston diameter of 40 mm, a piston rod diameter of 12 mm, and a maximum pressure of 10 bar as the load-setting element. To repeat the test carried out previously by the FEM method and properly reproduce the load of the element on the surface of a circle with a diameter of 50 mm, a stamp of the appropriate size and mounting was 3D printed. In addition, the stand included a Pneumax pressure regulator, a Festo valve, and an HBM load cell used to accurately read the force applied to the specimen during the test. The specimen was supported on two metal cylinders at a distance of 10 mm from the edge of the specimen.

An MGCplus controller and HBM software were used as control and result reading software. The data collecting system was MGCplus AB22A of the German company HBM. The device is able to connect up to 6 expansion cards. In our case, the ML455i and ML801b cards were used to collect data. The HBM U2B force sensor with a measuring range of 0-500N was connected

to the ML455i card. A strain gauge with the previously specified parameters has been connected to the ML801b card.

Each sample was loaded with a force of 200 N. The results were collected on the computer with CatmanEasy software.

2.5. Material's Model Definition

Based on the results obtained during the test strain gauge testing, the boundary conditions were recreated in ANSYS Workbench 19.2 software to determine material parameters (Young's modulus) for each sample. The samples are described in chapters 2.2 and 2.3.

Additional layers on the top and bottom surfaces with a thickness of 1 mm were added to the sample models previously described in Section 2.2. These layers represent the additional resin layers that were tested during the previous test. The boundary conditions (restraint and specimen loading) remained the same from the initial FEA analysis.

The PLA material model was modified so that the strain results obtained correspond to those obtained in the strain gauge test. The value of Young's modulus was modified to value of 1.55 GPa. Three additional material models were introduced for resins with different reinforcing additives (LG 700 epoxy resin, resin with 10% and 20% addition of carbon fiber powder). For each resin, a density of 0.65 g/cm3 and a Poisson ratio of 0.33 were assumed. Young's modulus was left as the only variable.

The Young's modulus value for each material was then modified to replicate the results read at the strain gauge restraint in the previous test.

2.6. FEM Analysis of the Driver Seat

Although the elementary unit is very similar to an ordinary lattice structure, its parameterization and the ability to arrange it freely gives it a number of advantages - for example, the ability to lay out the elements along a curve, which allows the elementary units to fit a given geometry. This property makes it possible to arrange them in such a way that the applied load on the top surface is always perpendicular to the direction in which the units present the greatest strength - such an arrangement is not possible using a standard lattice fill pattern. This solution has been presented in Figure 7. In standard lattice structures, there are greater chances of shear stresses occurring. This feature allows the use of sandwich-type structures also for the manufacture of components that are not perfectly flat, unlike the structures currently in use.

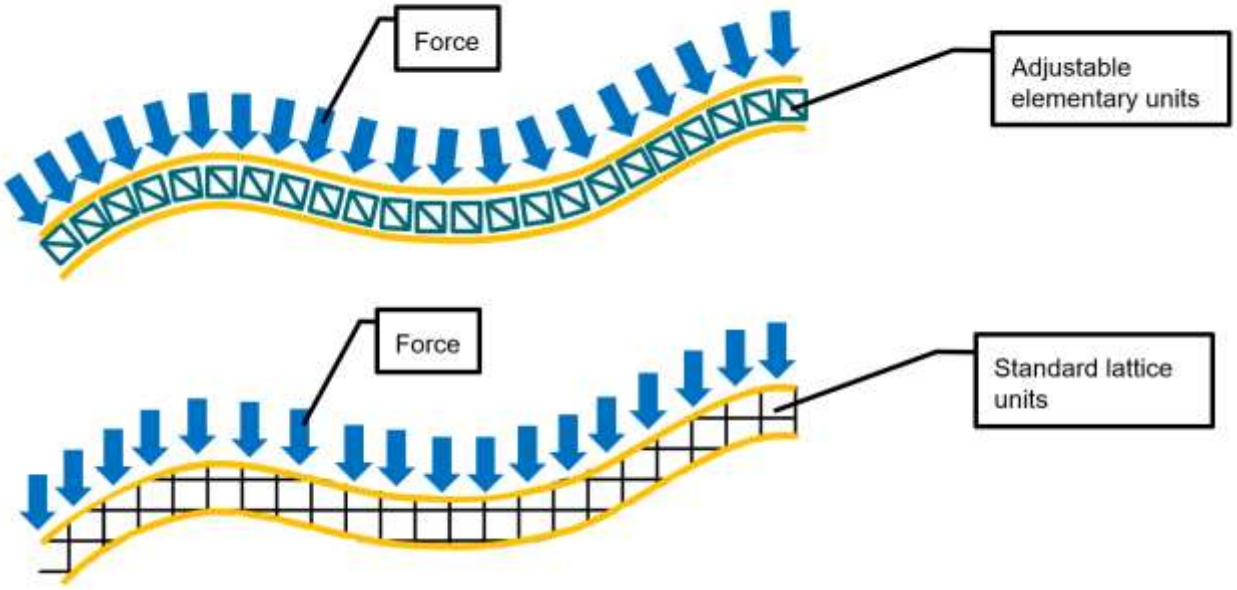

Figure 7: *Advantages of adjustable elementary units [own illustration]*

In the final stage of the research, in order to verify the application of the previously presented elements and structures, a section of the driver's seat for the Greenpower electric car was designed. The model was created with Siemens NX 12 software using all the assumptions and elements presented in the previous chapters. The seat consisted of a core of 3,000 elements with Structure B and two outer layers of 0.5 mm thick-ness representing epoxy resin with the addition of 20% carbon fiber powder. The application of the driver's seat model (marked in blue) in the car is presented in the Figure 8 below.

Figure 8: *Application of the Driver's Seat in Green Power Car [own illustration]*

Next, an FEA analysis of the designed seat was carried out in ANSYS Workbench 19.2. Because the component is symmetric, only half of the model was used for the analysis to reduce the calculation time. PLA material was assigned for the core elements, while epoxy resin with 20% carbon fiber powder was assigned for the outer layers. A model mesh was created with an element size of 4 mm for the outer layers. The model was fixed in two areas: on the bottom surface representing the attachment of the seat to the floor of the car, and on an additional edge simulating the support of the seat under the back. The boundary conditions of the model are shown in Figure 9.

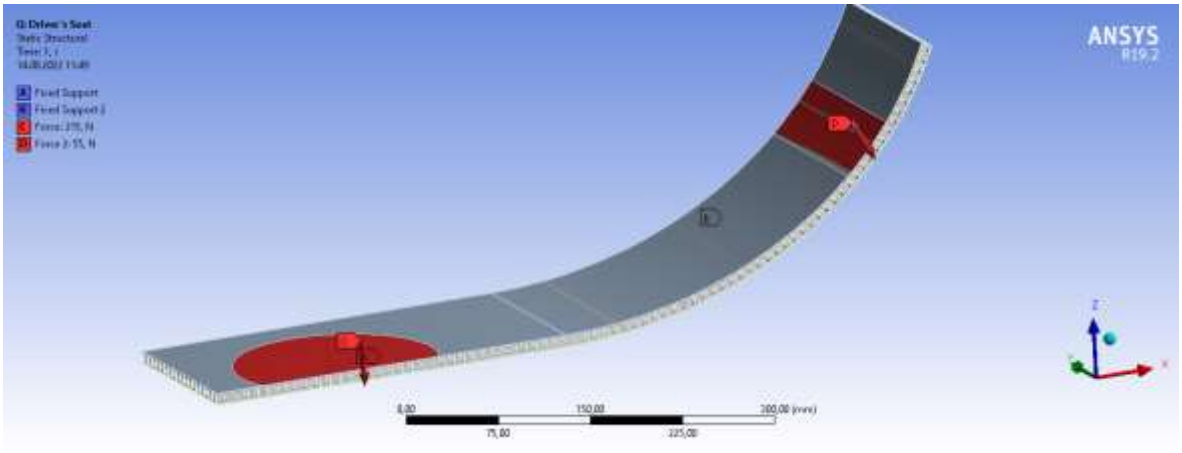

Figure 9: *Boundary conditions for FEM analysis of the Greenpower driver's seat [own illustration]*

The seat was loaded with two forces representing the pressure caused by the driver's own weight. The driver's weight was taken as 63 kg, as an average weight of the drivers who drove the car in the last season. The lower surface of the seat is affected by 68% of the weight, that is, 43 kg, and the part below the back is affected by 17%, that is, 11 kg. Since only half of the seat was analyzed in the model, half of the forces corresponding to each weight - 215 N and 55 N - were taken as loads.

3. Results

This section successively describes the results from the Finite Element Method analysis carried out in Ansys Workbench 19.2 software and results from the strain gauge testing.

3.1. Finite Element Analysis

As a result of the numerical Finite Element Method analysis carried out in the Siemens NX software, the values of deformation and von Mises stress for each core structure sample have been obtained. The results acquired for each sample type are presented in Table 4.

Table 4: *Results of FEM analysis for each sample type [own source]*

	Structure A	Structure B	Structure C	Structure D
von Mises stress [MPa]	23.89	17.43	16.63	11.86
Strain [mm/mm]	$9.05 \cdot 10^{-3}$	$6.71 \cdot 10^{-3}$	$6.30 \cdot 10^{-3}$	4.55·10-3
Deformation [mm]	1.76	1.06	0.91	0.36

It can be noted that both factors – the diagonal support and layering of elementary units had significant influence on the results. The stresses in Structure A with one layer of elementary units without diagonal support were 23.89 MPa, while the strain value was $9.05 \cdot 10^{-3}$ mm/mm and deformation was 1.76 mm. For Structure B with one layer and diagonal support, the values were 17.43 MPa, $6.71 \cdot 10^{-3}$ mm/mm and 1.06 mm, respectively. The stresses in Structure B compared to Structure A are 27% lower, while the strain is 26% lower and deformation is 40% lower. The results for Structure B are shown in Figure 10.

For Structure C with two layers of elementary units without diagonal support, the stress was 16.63 MPa, strain 6.30·10-3 mm/mm and the deformation was 0.91 mm. Stress in Structure C is 30% less than in Structure A, but only 5% greater than in Structure B. Strain value is 30% lower than for Structure A and only 6% lower than for Structure B. Deformation, on the other hand, is 48% less than in Structure A and 14% less than in Structure B. For Structure D with two layers of reinforced units, the stress was 11.86 MPa, so 27% less than in Structure C and 32% less than in Structure B. Strain value was $4.55 \cdot 10^{-3}$ mm/mm, so 32% lower than for Structure B and 28% lower than for Structure C. The deformation in Structure D was 0.36 mm, so 60% less than in Structure C and 66% less than in Structure B.

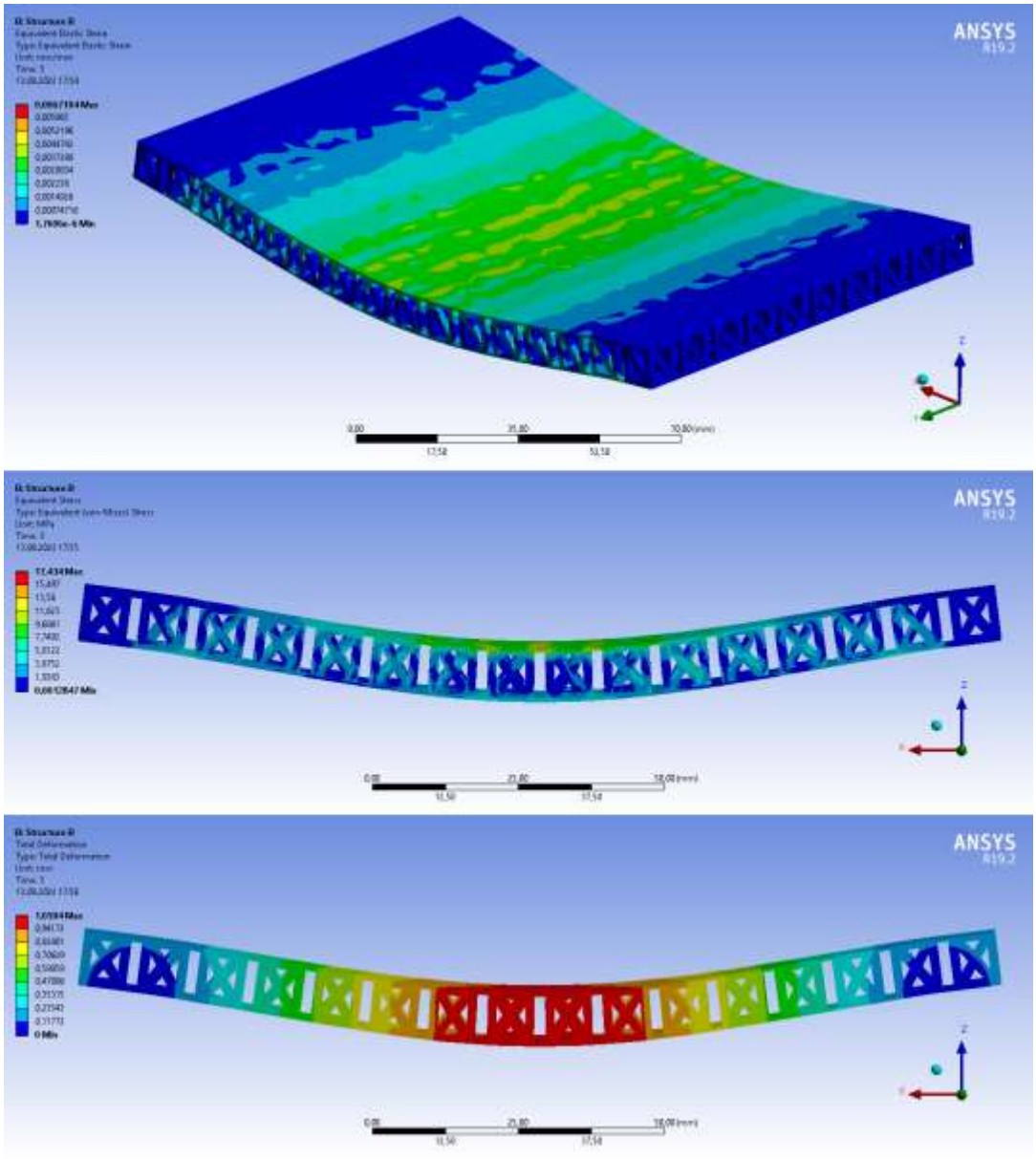

Figure 10: *FEM results for Structure C – above: strain results, middle: von Mises stress results, be-low: deformation results [own illustration]*

From the information above, it can be concluded that it is more advantageous to use a core with one layer, but with an additional diagonal support than two layers without this support; then we obtain only 5% greater stresses and 6% greater strain values, while maintaining 19% less element weight. An additional layer of reinforced elements reduced stress and strain values by 32%, while deformation was reduced by more than 60%.

3.2. Strain Gauge Testing

When the samples were loaded with a force of 200 N, readings were obtained from strain gauges attached to the bottom of the samples. The readings for each sample are shown in Table 5 below.

Table 5: *Strain readings [mm/mm] of strain gauge test for each sample [own source]*

	Sample 1	**Sample 2**	**Sample 3**	**Sample 4**
100 N	$1.9 \cdot 10^{-3}$	$1.63 \cdot 10^{-3}$	$1.45 \cdot 10^{-3}$	$9.2 \cdot 10^{-4}$
150 N	-	$2.46 \cdot 10^{-3}$	$2.17 \cdot 10^{-3}$	$1.31 \cdot 10^{-3}$
200 N	-	$3.55 \cdot 10^{-3}$	-	$1.79 \cdot 10^{-3}$
	Sample 5	**Sample 6**	**Sample 7**	**Sample 8**
100 N	$9.3 \cdot 10^{-4}$	$6.47 \cdot 10^{-4}$	$7.25 \cdot 10^{-4}$	$4.96 \cdot 10^{-4}$
150 N	$1.24 \cdot 10^{-3}$	$9.29 \cdot 10^{-4}$	$1.08 \cdot 10^{-3}$	$8.11 \cdot 10^{-4}$
200 N	-	$1.22 \cdot 10^{-3}$	-	$1.16 \cdot 10^{-3}$

From the table above, it can be seen that none of the samples with Structure A core (Samples 1, 3, 5 and 7) reached a force of 200 N - the failure of the samples occurred earlier. Sample 1 without reinforcement of any resin layer did not even reach 150 N. The diagonal support gives a noticeable strengthening of the entire structure - all samples reached a force of 200 N, even Sample 2 without resin layers.

From the reading for a force of 200 N, it can be seen that a layer of pure epoxy res-in gives a stiffening of the structure, and thus less deformation by 50% compared to PLA alone. It can also be noted that the 10% addition of carbon fiber powder reduces deformation relative to pure epoxy resin by 32% and relative to PLA alone by up to 66%. The addition of 20% powder reduced strain relative to the 10% addition by only 5%.

Based on the results, the stiffness of each sample was calculated using Equation (1),

$$k = \frac{F}{\delta} \quad (1)$$

where:

F [N] – force acting on the body,

δ [mm] – the displacement produced by the force in the same direction.

A graph was then drawn to show the change in stiffness of the specimen depending on the type of structure as well as the addition of the laminate layer. The results are shown in Figure 11.

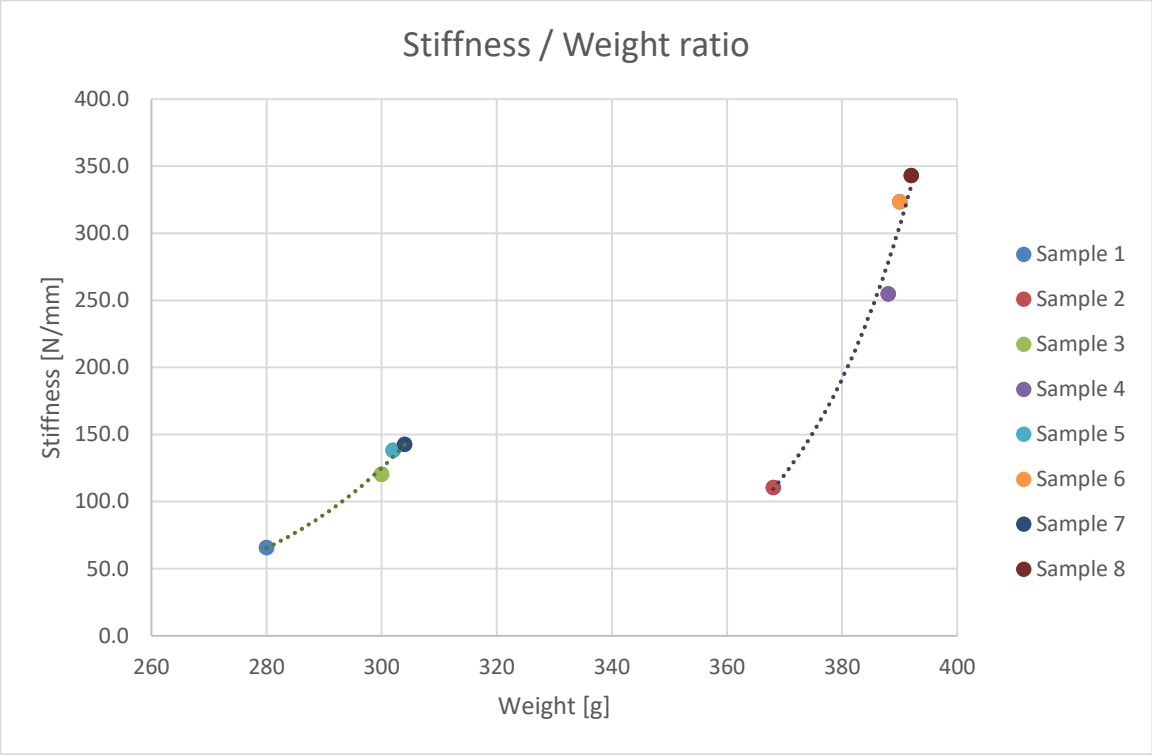

Figure 11: *Stiffness to weight ratio of each sample [own source]*

In the graph, it can be seen that samples having Structure A are characterized by lower weight, but also lower stiffness reaching an average value of 117 N/mm (points on the left side of the graph). Samples having Structure B are characterized by a higher weight, but also significantly higher stiffness reaching an average value of 258 N/mm (points on the right side of the graph). The average stiffness of samples with Structure B is as much as 120% higher than those with Structure A.

3.3. Material's Model Definition

Based on the reproduction of the results and readings from the strain gauges de-scribed in Section 3.2, the material properties for layers of epoxy resin and resin with carbon fiber powder additives were defined. The value of Young's modulus was adjusted to obtain the strain values previously read from the strain gauges. The Figure 12 shows the results obtained for Sample 8. Result probes were placed around the place where the strain gauge was mounted on the sample. The 4 probes indicated a result of about 1.16·10-3 mm/mm, which was the target value for this sample.

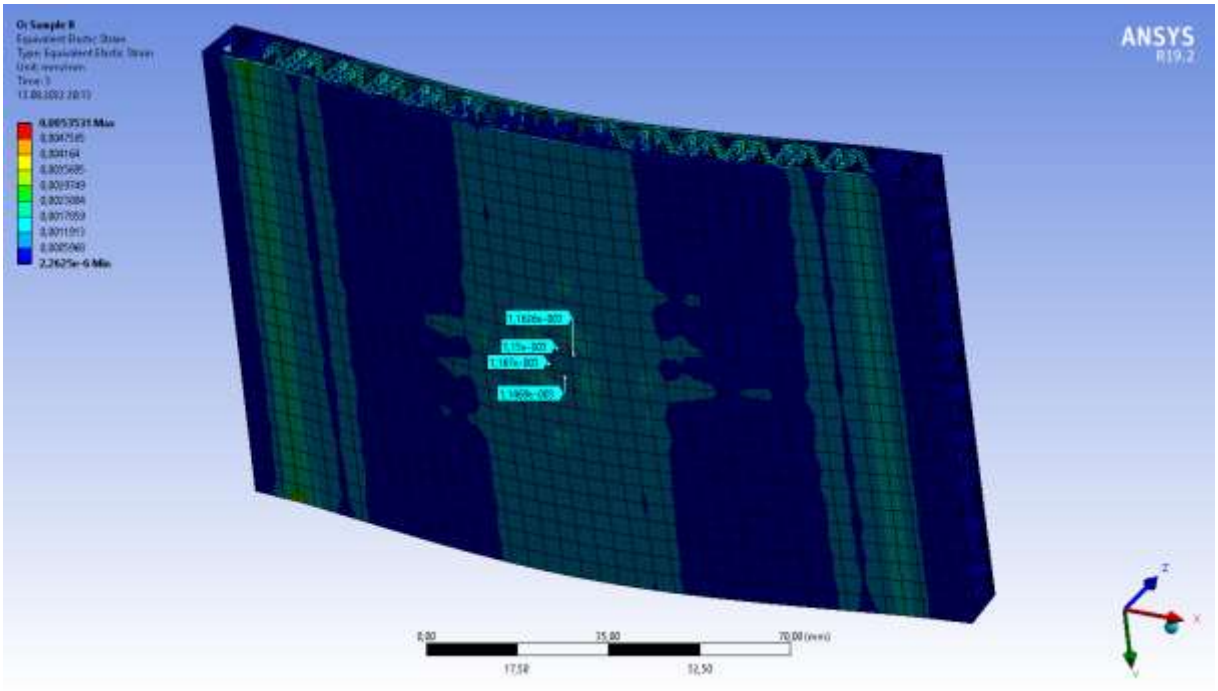

Figure 12: *Strain results for Sample 8 [own illustration]*

The density of the defined resin was calculated at 0.65 g/gm3, while the Poisson ratio was 0.33. The Young's modulus for each additive layer material is presented in Table 6.

Table 6: *Young's Modulus values obtained for each material [own source]*

Material	**Young's Modulus [GPa]**
No coating PLA	1.55
Pure epoxy resin LG700	1.20
LG700 + 10% carbon fiber powder	2.00
LG700 + 20% carbon fiber powder	2.25

From the above, it can be seen that the addition of carbon fiber powder to epoxy resin has a significant effect on raising the Young's modulus of the resulting material. The Young's modulus of the resin with 10% addition of carbon fiber powder is 67% higher than that of pure epoxy resin. On the other hand, the Young's modulus of the resin with 20% addition is 12.5% greater than that of the resin with 10% powder addition.

3.4. FEM Analysis of the Driver's Seat

FEA analysis resulted in von Mises-reduced stresses and deformation in the model. The results are shown in Figure 13 below.

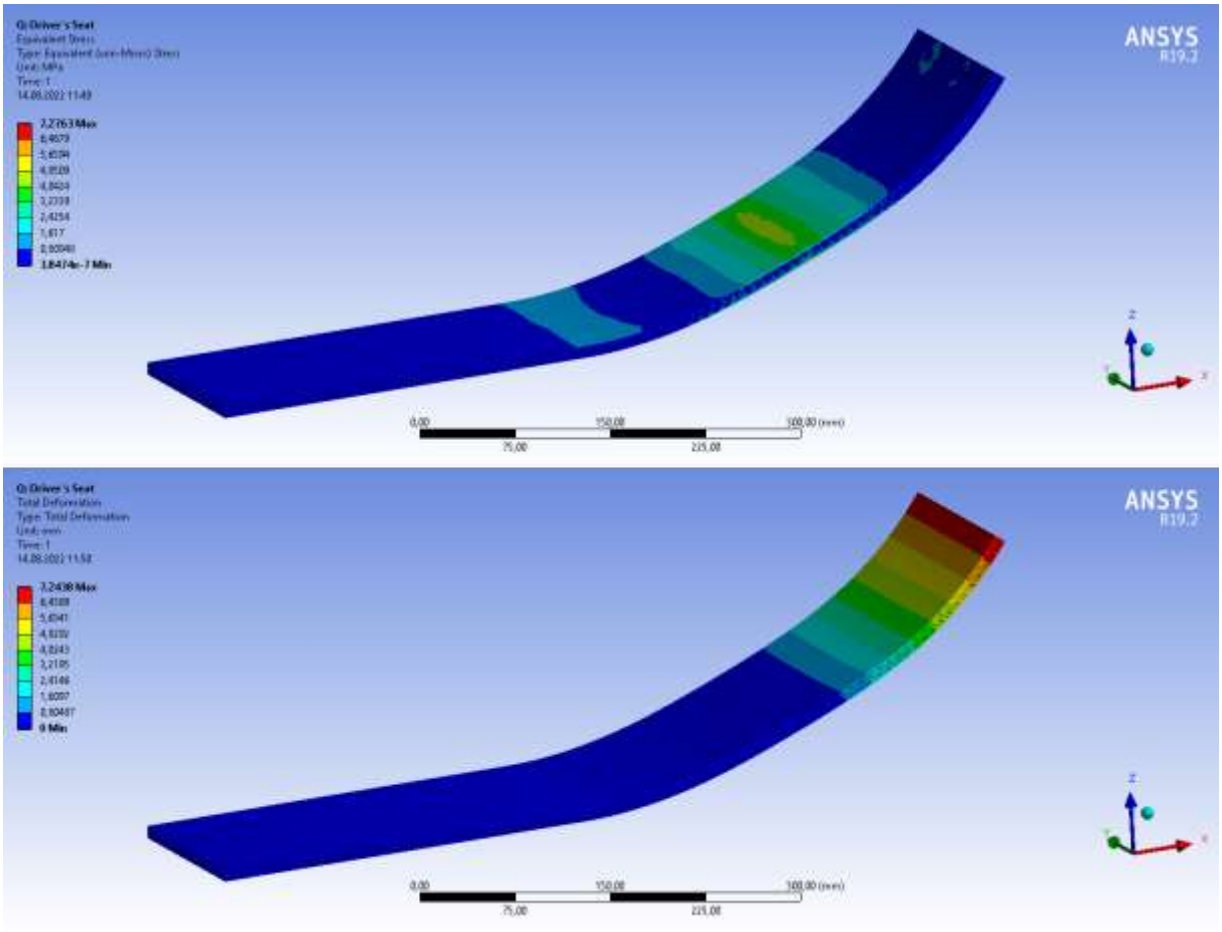

Figure 13: *FEM results for driver's seat – top: von Mises stress, bottom: deformation [own illustration]*

The maximum stress was 7.28 MPa and occurred in the core structure in the back support area. The stresses did not exceed the permissible values. The maximum de-formation was 7.24 mm. The obtained results imply, that they do not exceed safe values for these materials, that is tensile strength, and can be adopted as a seat material.

It should be noted that the seat designed in this way reduces the weight of the component by 172 g, a reduction of about 25% compared to a seat made entirely of PLA.

Covering the driver's seat with a layer of epoxy resin laminate with the addition of carbon fiber powder provides sufficient strength to the component, while the ability to 3D print makes it possible to produce a personalized part for Greenpower's small electric car.

4. Discussion and Conclusion

In the above article, the authors presented novel CFRP sandwich structures using FDM 3D printing. The design of a scalable elementary unit used in an FDM printed core is presented. Two concepts of the elemental unit in a truss concept were presented - a simple one and one with an additional diagonal support. During further testing - both FEA and experimental by strain gauging, it was observed that the diagonal support significantly increases the strength of the elementary unit as well as the entire structure in which it is used.

During the initial FEA analysis, the properties of the structures were verified, and the possible benefits of successive layers of elementary units in the core were examined.

In the following section, a method for manufacturing such structures is presented - 3D printing in FDM technology of a core of thermoplastic material, and then coating its outer layers with resin. Three different coating materials were tested - pure epoxy resin, resin with the addition of 10% and 20% carbon fiber powder.

In an experimental study on a resistance strain gauge bench, the behavior of the structures under a force of 200 N was checked, as well as what deformations occur on the bottom surface of the component. From the results collected for a force of 200 N, it can be seen that a layer of pure epoxy resin gives a stiffening of the structure and thus less deformation by 50% compared to PLA alone. It was noted that 10% addition of carbon fiber powder reduces deformation relative to pure epoxy resin by 32%, and relative to PLA alone by as much as 66%. The addition of 20% powder reduced strain relative to the 10% addition by only 5%. The average stiffness of samples with Structure B is as much as 120% higher than those with Structure A.

With the results collected, material parameters were reconstructed for individual layers of resin with additives, allowing these material models to be used in computerized strength testing of more complex geometries and components. As an example of the use of both the 3D printed CFRP sandwich structure fabrication technology with carbon fiber powder and the top layer material model, an FEM strength analysis of the Greenpower electric car driver's seat was conducted.

In future studies, the authors plan to test other designed core structures produced using the technology described above and to test yet more coating materials.

REFERENCES

Alshaer, A. W., & Harland, D. J. An investigation of the strength and stiffness of weight-saving sandwich beams with CFRP face sheets and seven 3D printed cores. Composite Structures, 2021, 257, 113391. https://doi.org/10.1016/j.compstruct.2020.113391

Audibert, C., Chaves-Jacob, J., Linares, J. M., & Lopez, Q. A. Bio-inspired method based on bone architecture to optimize the structure of mechanical workspieces. Materials & Design, 2018, 160, 708-717. https://doi.org/10.1016/j.matdes.2018.10.013

Baier, A., Zur, P., Kolodziej, A., Konopka, P., & Komander, M. Studies on optimization of 3D-printed elements applied in Silesian Greenpower vehicle. In IOP Conference Series: Materials Science and Engineering, 2018, 400(2), 022010. https://doi.org/10.1088/1757-899X/400/2/022010

Bodaghi, M., Serjouei, A., Zolfagharian, A., Fotouhi, M., Rahman, H., & Durand, D. Reversible energy absorbing meta-sandwiches by FDM 4D printing. International Journal of Mechanical Sciences, 2020, 173, 105451. https://doi.org/10.1016/j.ijmecsci.2020.105451

Dey, A., & Yodo, N. A systematic survey of FDM process parameter optimization and their influence on part characteris-tics. Journal of Manufacturing and Materials Processing, 2019, 3(3), 64. https://doi.org/10.3390/jmmp3030064

Dudek, P. F. D. M. FDM 3D printing technology in manufacturing composite elements. Archives of metallurgy and materials, 2013, 58(4), 1415-1418. https://doi.org/10.2478/amm-2013-0186

Dudescu, C., & Racz, L. Effects of raster orientation, infill rate and infill pattern on the mechanical properties of 3D printed materials. ACTA Univ. Cibiniensis, 2017, 69(1), 23-30. https://doi.org/10.1515/aucts-2017-0004

Fernandez-Vicente, M., Calle, W., Ferrandiz, S., & Conejero, A. Effect of infill parameters on tensile mechanical behavior in desktop 3D printing. 3D printing and additive manufacturing, 2016, 3(3), 183-192. https://doi.org/10.1089/3dp.2015.0036

Fiał, C., & Pieknik, M. Druk 3D jako technologia przyszłości–część 1. Technologia i Jakość Wyrobów, 2020, 65.

Garzon-Hernandez, S., Garcia-Gonzalez, D., Jérusalem, A., & Arias, A. Design of FDM 3D printed polymers: An experi-mental-modelling methodology for the prediction of

mechanical properties. Materials & Design, 2020, 188, 108414. https://doi.org/10.1016/j.matdes.2019.108414

Hao W., Liu Y., Zhou, Chen H. H., Fang D.: Preparation and characterization of 3D printed continuous carbon fiber rein-forced thermosetting composite, Polymer Testing 65, 2018, p. 29-34. https://doi.org/10.1016/j.polymertesting.2017.11.004

Hu, T., Wang, J., Wang, J., & Chen, R. Electromagnetic interference shielding properties of carbonyl iron powder-carbon fiber felt/epoxy resin composites with different layer angle. Materials Letters, 2015, 142, 242-245. https://doi.org/10.1016/j.matlet.2014.12.026

Khosravani, M. R., Zolfagharian, A., Jennings, M., & Reinicke, T. Structural performance of 3D-printed composites under various loads and environmental conditions. Polymer testing, 2020, 91, 106770. https://doi.org/10.1016/j.polymertesting.2020.106770

Kołodziej, A.; Żur, P.; Borek, W. Influence of 3D-printing Parameters on Mechanical Properties of PLA defined in the Static Bending Test. Eur. J. Eng. Sci. Technol. 2019, 2, 65–70.

Kowalewski Z., Szymczak T., Podstawy tensometrii elektrooporowej oraz praktyczne jej zastosowania, Dziewiętnaste Se-minarium Nieniszczące Badania Materiałów Zakopane, Poland, 12-13 March 2013

Kwon, D. J., Kim, J. H., DeVries, K. L., & Park, J. M. Optimized epoxy foam interface of CFRP/Epoxy Foam/CFRP sandwich composites for improving compressive and impact properties. Journal of Materials Research and Technology, 2021, 11, 62-71. https://doi.org/10.1016/j.jmrt.2021.01.015

Lalegani Dezaki, M., & Mohd Ariffin, M. K. A. The effects of combined infill patterns on mechanical properties in FDM process. Polymers, 2020, 12(12), 2792. https://doi.org/10.3390/polym12122792

Lionetto, F., Moscatello, A., & Maffezzoli, A. Effect of binder powders added to carbon fiber reinforcements on the chemoreology of an epoxy resin for composites. Composites Part B: Engineering, 2017, 112, 243-250. https://doi.org/10.1016/j.compositesb.2016.12.031

Liu, Z., Lei, Q., & Xing, S. Mechanical characteristics of wood, ceramic, metal and carbon fiber-based PLA composites fabricated by FDM. Journal of Materials Research and Technology, 2019, 8(5), 3741-3751. https://doi.org/10.1016/j.jmrt.2019.06.034

Lubombo, C., & Huneault, M. A. Effect of infill patterns on the mechanical performance of lightweight 3D-printed cellular PLA parts. Materials Today Communications, 2018, 17, 214-228. https://doi.org/10.1016/j.mtcomm.2018.09.017

Mazzanti, V., Malagutti, L., & Mollica, F. FDM 3D printing of polymers containing natural fillers: A review of their mechan-ical properties. Polymers, 2019, 11(7), 1094. https://doi.org/10.3390/polym11071094

Mei, J., Liu, J., & Huang, W. Three-point bending behaviors of the foam-filled CFRP X-core sandwich panel: Experimental investigation and analytical modelling. Composite Structures, 2022, 284, 115206. https://doi.org/10.1016/j.compstruct.2022.115206

Mei, J., Tan, P. J., Bosi, F., Zhang, T., Liu, J. Y., Wang, B., & Huang, W. Fabrication and mechanical characterization of CFRP X-core sandwich panels. Thin-Walled Structures, 2021, 158, 107144. https://doi.org/10.1016/j.tws.2020.107144

Melnikova, R., Ehrmann, A., & Finsterbusch, K. 3D printing of textile-based structures by Fused Deposition Modelling (FDM) with different polymer materials. IOP conference series: materials science and engineering, 2014, 62(1), 012018. https://doi.org/10.1088/1757-899X/62/1/012018

Miłek, M. Metrologia elektryczna wielkości nieelektrycznych. Uniwersytet Zielonogórski, Zielona Góra, Poland, 2006

Nowak, A., Baier, A., Kołodziej, A., & Żur, P. (2021, October). Race car mirror cover production focused on reducing air drag. IOP Conference Series: Materials Science and Engineering, 2021, 1182(1), 012055. https://doi.org/10.1088/1757-899X/1182/1/012055

Podroužek, J., Marcon, M., Ninčević, K., & Wan-Wendner, R. Bio-inspired 3D infill patterns for additive manufacturing and structural applications. Materials, 2019, 12(3), 499. https://doi.org/10.3390/ma12030499

Popescu, D., Zapciu, A., Amza, C., Baciu, F., & Marinescu, R. FDM process parameters influence over the mechanical properties of polymer specimens: A review. Polymer Testing, 2018, 69, 157-166. https://doi.org/10.3390/ma12030499

Sajadi, S. M., Owuor, P. S., Schara, S., Woellner, C. F., Rodrigues, V., Vajtai, R., ... & Ajayan, P. M. Multiscale geometric design principles applied to 3D printed schwarzites. Advanced Materials, 2018, 30(1), 1704820. https://doi.org/10.1002/adma.201704820

Saufi, S. A. S. A., Zuhri, M. Y. M., Dezaki, M. L., Sapuan, S. M., Ilyas, R. A., As' arry, A., ... & Bodaghi, M. Compression Behaviour of Bio-Inspired Honeycomb Reinforced Starfish Shape Structures Using 3D Printing Technology. Polymers, 2021, 13(24), 4388. https://doi.org/10.3390/polym13244388

Schmitt, M., Mehta, R. M., & Kim, I. Y. Additive manufacturing infill optimization for automotive 3D-printed ABS components. Rapid Prototyping Journal, 2019. https://doi.org/10.1108/RPJ-01-2019-0007

Sebaey, T. A., & Mahdi, E. Crushing behavior of a unit cell of CFRP lattice core for sandwich structures' application. Thin-Walled Structures, 2017, 116, 91-95. https://doi.org/10.1016/j.tws.2017.03.016

Solomon, I. J., Sevvel, P., & Gunasekaran, J. A review on the various processing parameters in FDM. Materials Today: Proceedings, 2021, 37, 509-514. https://doi.org/10.1016/j.matpr.2020.05.484

Tao, Y., Li, P., Zhang, H., Shi, S. Q., Zhang, J., & Yin, Q. Compression and flexural properties of rigid polyurethane foam composites reinforced with 3D-printed polylactic acid lattice structures. Composite Structures, 2022, 279, 114866. https://doi.org/10.1016/j.compstruct.2021.114866

Tian, X., Liu, T., Yang, C., Wang, Q., & Li, D. Interface and performance of 3D printed continuous carbon fiber reinforced PLA composites. Composites Part A: Applied Science and Manufacturing, 2016, 88, 198-205. https://doi.org/10.1016/j.compositesa.2016.05.032

Vedrtnam, A. Novel method for improving fatigue behavior of carbon fiber reinforced epoxy composite. Composites Part B: Engineering, 2019, 157, 305-321. https://doi.org/10.1016/j.compositesb.2018.08.062

Zhang, G., Ma, L., Wang, B., & Wu, L. Mechanical behaviour of CFRP sandwich structures with tetrahedral lattice truss cores. Composites Part B: Engineering, 2012, 43(2), 471-476. https://doi.org/10.1016/j.compositesb.2011.11.017

Zhang, J., & Yanagimoto, J. Design of bendable sandwich sheets with 3D printed CFRP cores via multi-stage topology optimization. Composite Structures, 2022, 287, 115372. https://doi.org/10.1016/j.compstruct.2022.115372

Żur, A., Żur, P., Michalski, P., & Baier, A. Preliminary Study on Mechanical Aspects of 3D-Printed PLA-TPU Composites. Materials, 2022, 15(7), 2364. https://doi.org/10.3390/ma15072364

Żur, P., Kołodziej, A., & Baier, A. Finite elements analysis of PLA 3D-printed elements and shape optimization. European Journal of Engineering Science and Technology, 2019, 2(1), 59-64. https://doi.org/10.33422/EJEST.2019.01.51

Żur, P., Kołodziej, A., Nowak, A., & Baier, A. Manufacturing A Personalised Composite Material Driver's Seat. International Journal of Modern Manufacturing Technologies, 2021, 13(3), 191-196. https://doi.org/10.54684/ijmmt.2021.13.3.191

http://www.grm-systems.cz/pl/epoxy [Accessed 7.09.2022]

https://www.easycomposites.eu/milled-carbon-fibre-powder [Accessed 7.09.2022]